A pixelated polarizer-based camera for instantaneous interferometric measurements

Neal J. Brock*, Bradley T. Kimbrough, James E. Millerd
4D Technology Corporation, 3280 E. Hemisphere Loop Unit 146, Tucson, AZ, USA 85706-5039

ABSTRACT

A pixel-level micropolarizer array bonded to a scientific camera has been developed for use in commercial dynamic interferometers. The pixelated array includes the 0, 45, 90, and, 135 degree polarization orientations. Micropolarizer arrays with elements as small as 7.4 microns and array sizes as large 4 Mega-pixels have been fabricated for use across the visible spectrum. The pixelated polarization camera acquires the four polarization orientations in a single video frame, which enables instantaneous interferometric or polarimetric measurements. Examples of each type of measurement are presented. Details of how the pixelated camera is used in interferometry are reviewed and the spatial resolution performance of the camera when used in interferometry is discussed.

Keywords: dynamic interferometry, micropolarizer array, pixelated polarizer, snap shot imaging polarimeter, spatial phase shifting, wiregrid

1. INTRODUCTION

Optical metrology has become an indispensable tool to engineers and scientists working at the forefront of technology where there is a relentless demand for better measurement capabilities. The demand for greater spatial and temporal resolution in imaging polarimeters and imaging interferometers inspired the development of micropolarizer arrays capable of matching the size and pitch of camera sensors. The concept of a pixel-matched polarizer array was described by Chun, *et. al.* in 1994 for use at infrared wavelengths.[1] The approach permits single frame, quantitative measurements without the deleterious effects of vibration and motion. Compared with multi-camera imaging, the pixel-matched polarizer is very compact and permits the use of conventional lenses where the optics can be very close to the sensor. A camera with a pixel-matched micropolarizer array was demonstrated in 1999 by Nordin[2] *et. al.*, where it was used in an imaging polarimetry system. Later, Millerd[3] *et. al.* developed a pixelated camera for use in a dynamic imaging interferometry system. Since then, the pixelated polarizer camera (also known as the pixelated phase camera) has been the core technology element to 4D Technology's commercial dynamic interferometers where it has been used for making dynamic phase measurements since 2004. With hundreds of systems installed in facilities around the world, it has proven to be a rugged and reliable platform. The pixelated cameras are used in a variety of commercial interferometers that are used primarily for measuring the shape and surface texture of optics and precision engineered surfaces. Researchers have applied other pixelated polarization cameras to imaging polarimetry applications such as 3D imaging, remote sensing, target discrimination, haze removal, bio-tissue imaging, and polarization microscopy.[4] In this paper we review details of 4D Technology's pixelated polarizer camera, discuss how it is used in dynamic interferometry systems, and present some examples of different types of polarimetric and phase measurements.

2. PIXELATED POLARIZER CAMERA

The pixelated polarizer technology used in interferometry was co-developed by 4D Technology Inc. and Moxtek Inc. The micropolarizer arrays utilize Moxtek's wiregrid polarizer technology which utilizes nanoscale patterning to form a metal grating with sub-wavelength spacing on a thin transparent glass substrate. The wiregrid polarizer is characterized by high transmission, high extinction, and a broad spectral and angular bandwidth. The wiregrid micro-polarizer array is produced in a multi-step lithographic process that produces a pattern of polarizers with four discrete polarizations (0, 45, 90, 135 degrees) known as a super pixel (see Figure 1) that is repeated over the entire array. The size and frequency or spacing of the individual micropolarizer element is chosen to match exactly the size and pitch of the desired camera

* neal.brock@4DTechnology.com, phone 520-294-5600, 4DTechnology.com

sensor. Polarization crosstalk is kept to a minimum by leaving an unpatterned border area around each individual polarizer element and by mounting the micropolarizer substrate directly to the camera CCD microlens surface. Cross-talk can also be minimized by careful choice of the pixelated polarizer ordering. The polarizer ordering diagramed in Figure 1 was shown to minimize cross-talk for interferometry in reference 5 and for polarimeters in reference 6.

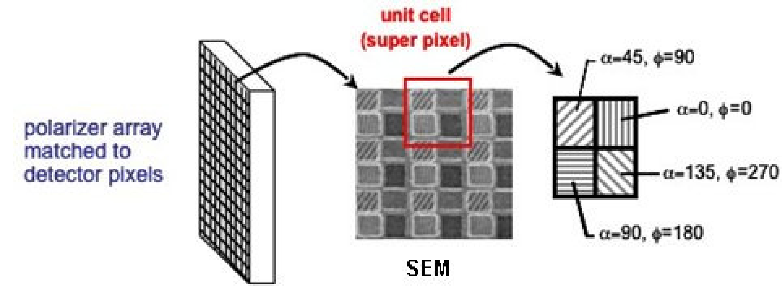

Figure 1. The diagram of the pixelated micropolarizer array shows the multiple polarization orientations that comprise the super pixel cell. The central image is an SEM of the micropolarizer array (courtesy of Moxtek Inc.).

The critical alignment and bonding of the micropolarizer array to the CCD is performed with a precision alignment station developed by 4D Technology. The micropolarizer array can be used over a wavelength range from 300nm to 3mm. At a wavelength of 550nm, the transmission of the pixelated polarizer can be as high as 80% and the extinction ratio can be greater than 50:1.[7] The cameras can be used with either coherent or incoherent light. Three standard pixelated cameras are available in the same physical housing (shown in Figure 2) with pixel resolutions of 1, 2, and 4 Megapixels. The cameras, utilize interline transfer CCD imaging sensors with 7.4 micron pixels and a CameraLink interface.

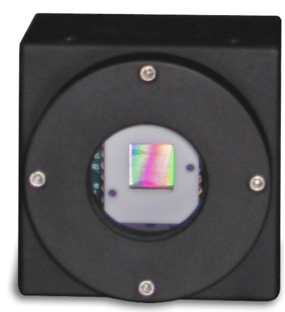

Figure 2. Compact 1Mpixel micropolarizer camera (57x57x46mm) with C-mount.

3. PHASE MEASUREMENT METHOD

In imaging polarimetry systems that employ pixelated micropolarizer cameras, the polarization data can be used to determine the Stokes parameters at each super pixel.[6] However, in interferometry systems the polarization data is used to determine the phase difference between a reference and test beam, which are orthogonally polarized. The principle behind the use of micropolarizer camera in interferometry is depicted in Figure 3. Kothiyal and Delisle[8] showed that the intensity of two beams having orthogonal circular polarization (i.e., right hand circular and left hand circular), which are interfered by a polarizer, is given by

$$I(x,y)=\frac{1}{2}\left(I_r+I_s+2\sqrt{I_rI_s}\cos\left(\Delta\phi(x,y)+2\alpha_p\right)\right) \quad (1)$$

where α_p is the angle of the polarizer with respect to the x, y plane. From this relation it can be seen that a polarizer oriented at zero degrees enables the in-phase (i.e., 0°) components of the incident reference and test wavefronts to interfere. A polarizer oriented at 45 degrees enables the in-phase quadrature (i.e., 90°) component between the incident reference and test wavefronts to interfere. A polarizer oriented at 90 degrees enables the out-of-phase (i.e., 180°) component between the incident reference and test wavefronts to interfere. Finally, a polarizer oriented at 135 degrees enables the out-of-phase quadrature (i.e., 270°) component between the incident reference and test wavefronts to interfere.

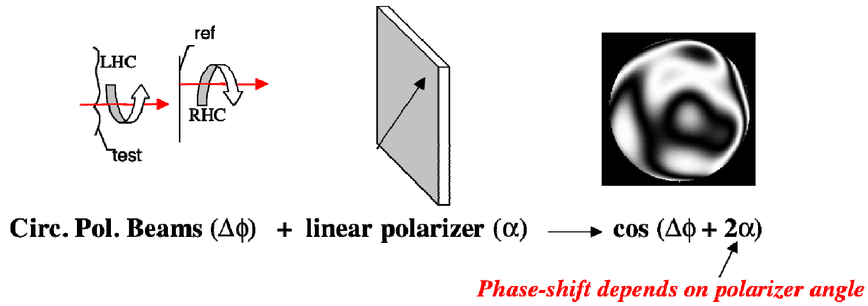

Figure 3. Diagram shows the phase shifting principle employed by micropolarizer array used in interferometry. Two oppositely circular polarized light beams are made linear by a polarizer. The resulting phase shift of the interfering beams is a function of the polarizer angle.

A diagram showing how a pixelated camera is used with a polarization interferometer to produce phase-shifted interferograms[9] is in Figure 4. A polarization interferometer generates a reference wavefront R and a test wavefront T having linear polarizations that are orthogonal with respect to each other. A quarter waveplate is used to convert the linearly polarized wavefronts R and T to left and right hand circular polarizations that subsequently interfere after transmitting the micropolarizer array. The sensor array converts the optical intensity at each pixel to an electrical charge. The micropolarizer array and the sensor array are located in substantially the same image planes. The data captured by the pixelated camera can be parsed into four sub-arrays corresponding to each of the four polarizations for display purposes. Each sub-array is a phase-shifted interferogram with a phase corresponding to the phase difference between the R and T wavefronts plus the discrete shift corresponding to its polarizer angle.

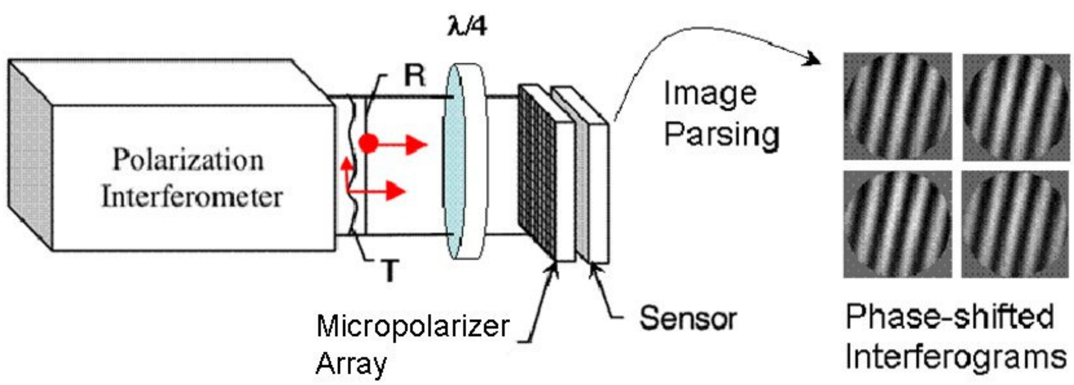

Figure 4. Diagram of micropolarizer array as it is used with polarization interferometer. Linearly polarized Reference and Test beams are circularized by a quarter waveplate before passing through micropolarizer array. Parsing the frames generates phase-shifted interferograms.

4. DATA PROCESSING

4.1 Phase Shift Interferometry

The phase-shifted interferograms are converted to quantitative phase data using Phase Shift Interferometry (PSI) algorithms as follows. The intensity (*I*) of each of the phase-shifted interferograms incident on the active surface of the detector array is given by:

$$I_0 = \frac{1}{2}\left(I_r + I_s + 2\sqrt{I_r I_s}\cos(\Delta\phi)\right), \tag{2}$$

$$I_1 = \frac{1}{2}\left(I_r + I_s + 2\sqrt{I_r I_s}\cos\left(\Delta\phi + \frac{\pi}{2}\right)\right), \tag{3}$$

$$I_2 = \frac{1}{2}\left(I_r + I_s + 2\sqrt{I_r I_s}\cos(\Delta\phi + \pi)\right), \tag{4}$$

$$I_3 = \frac{1}{2}\left(I_r + I_s + 2\sqrt{I_r I_s}\cos\left(\Delta\phi + \frac{3\pi}{2}\right)\right), \tag{5}$$

where I_r and I_s are the intensities of the reference and test wavefronts, respectively (the intensities are proportional to R^2 and S^2). This set of phase-shifted intensities I_0, I_1, I_2, and I_3 may be analyzed numerically using a number of algorithms to solve explicitly for the phase difference between the reference and test wavefronts.

Phase may be calculated based on a single frame of data using the following equation:

$$\Phi(x, y) = \arctan\left(\frac{I_3(x, y) - I_1(x, y)}{I_2(x, y) - I_0(x, y)}\right), \tag{6}$$

where I_0, I_1, I_2, and I_3 are the respective intensities of each of the phase-shifted interferograms. The variables x and y are the pixel coordinates. This method results in a phase map with a size equal to $1/4^{th}$ the raw data. A more sophisticated convolution approach is shown in section 4.3 that can be used to calculate the phase-map and retain the spatial sampling of the original data array[5]. For this method, it is not necessary to parse the data into sub-arrays.

4.2 Polarimetry

When the pixelated polarization camera is used as an imaging polarimeter, light is imaged directly on to the micropolarizer array. In the simplest configuration, the quarter waveplate shown in the interferometer in Figure 4 is not used. The Stokes vector describes the polarized light incident to the camera:

$$S = \begin{bmatrix} S_0 \\ S_1 \\ S_2 \\ S_3 \end{bmatrix} = \begin{bmatrix} I_0 + I_{90} \\ I_0 - I_{90} \\ I_{45} - I_{135} \\ I_{LHC} - I_{RHC} \end{bmatrix}, \tag{7}$$

where I_0, I_{90}, I_{45}, I_{135}, are the intensities of the linear polarization components 0, 90, 45, 135 degrees and I_{LHC}, I_{RHC} are the circular polarization components left hand circular, and right hand circular, respectively. The micropolarizer array described here can be used to determine S_0, S_1, S_2. Additional optical components such as a waveplate can be used to determine S_3; however, the simplicity and instantaneous imaging capability of the pixelated camera are usually sacrificed. The fraction of incident light intensity in the linear polarization states is the degree of linear polarization:

$$DoLP = \frac{\sqrt{S_1^{\ 2} + S_2^{\ 2}}}{S_0} \quad . \tag{8}$$

The pixelated camera offers an extremely simple configuration for measuring the instantaneous polarization data for determining DoLP, which is a significant advantage over other polarimetry methods.

4.3 Spatial Resolution

Calculation of the phase at each super pixel results in a phase map with ¼ of the raw data, as shown in Figure 5a, where A, B, C, and D represent the polarizations, 0, 45, 90, and 135 degrees respectively. However, it was shown in reference 5 that the phase can be effectively calculated at each pixel using different groupings of adjacent pixels. Thus, by convolving a 2x2 pixel kernel across the array as shown in Figure 5b, the spatial resolution of the data can be improved. A similar result was obtained in an imaging polarimeter with a micropolarizer array in reference 10 where it was shown that sampling errors could be completely eliminated.

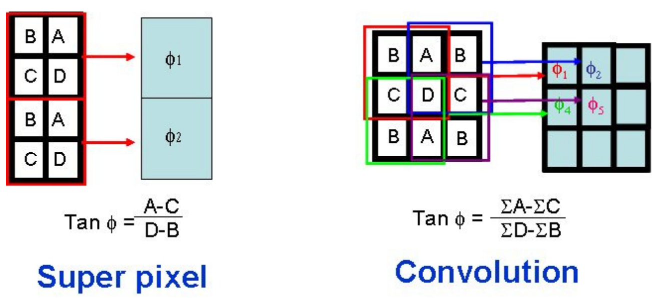

Figure 5. a) Diagram of micropolarizer super pixel and corresponding phase resolution. b) Diagram showing how 2x2 convolution kernel achieves higher resolution.

For an interferometric system measuring surface height, the instrument transfer function (ITF) is the ratio between the calculated surface height and the actual object surface height as a function of spatial frequency. In general, the instrument transfer function is not independent of the object being measured due to the non-linear nature of the interferometric process; however, for small surface height deviations it provides a sufficiently accurate metric for evaluation of the system performance. In order to determine the effect of the micropolarizer array sensor and associated algorithms on the ITF, a simulated step height measurement was performed. The simulation assumed a step height of 0.2 waves oriented along the y-axis. The imaging was strictly coherent with the system numerical aperture (NA) set to produce a cutoff frequency of ½ wave per pixel at the camera. The system was assumed to be diffraction limited. The camera sensor was simulated by an array of 1000 x 1000 pixels with 100% fill factor (i.e. there are no gaps between the pixels).

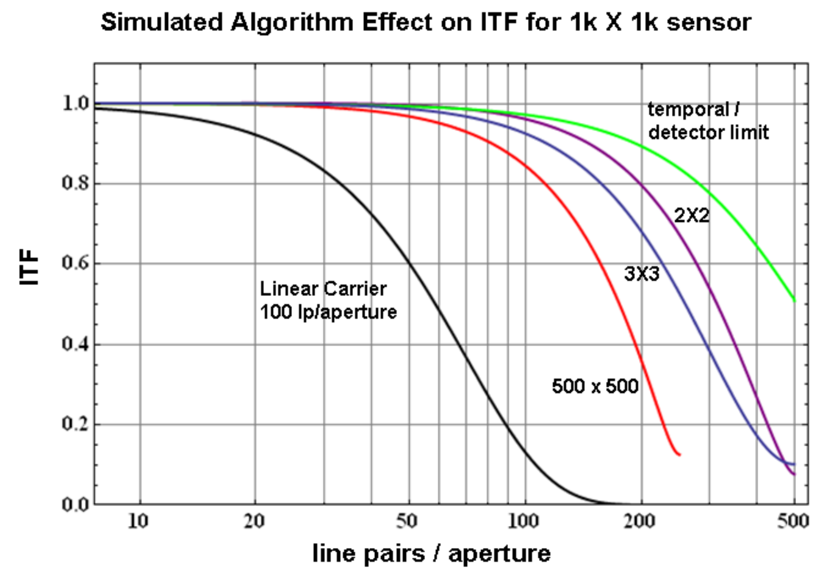

Figure 6. Instrument transfer function calculated for the pixelated mask sensor and associated algorithms. The calculation is based on a simulated 0.2 wave step measurement. The camera sensor is a 1000 x 1000 array of square pixels. The ITF of a temporal phase measurement, which is shown for comparison, is the limit due to the pixel width. The 500 x 500 trace represents the temporal ITF that would be obtained by an array with pixels twice as wide (i.e ¼ the number of pixels). The 2X2 and 3X3 traces show the response of the convolution method for the respective kernel sizes. The Linear Carrier trace shows the effective resolution of a Fourier Transform method utilizing 100 fringes of tilt as the carrier and a Gaussian filter.

These calculations show that using the convolution technique with the pixelated sensor preserves a significant portion of the spatial frequency spectrum. In this example for a 1000 x 1000 array, the curve labeled "temporal" is the maximum resolution that can be achieved, assuming a diffraction limited optical system and pixels with 100% fill factor. The curve labeled "500x500" represents the frequency response that would be achieved for an array with ¼ the number of pixels that are twice as wide (equal to 4 pixels of the 1000x1000 sensor). For the pixelated phase sensor, the 500x500 curve represents the resolution that would be achieved if the array was sub-divided into unique groups of 4 neighboring pixels, and a single phase value was calculated for each sub-group. Utilizing the convolution algorithm extends the frequency response out to the limit of the full sensor resolution, significantly beyond the 500 x 500 limit. Also shown for comparison in Figure 6 is the response of a phase measurement utilizing the spatial carrier method. 100 fringes of linear tilt are used to generate the carrier frequency on a 1000x1000 sensor. In this case, the ITF is significantly limited by the frequency response of the spatial carrier processing filter.

5. RESULTS

Pixelated polarizer cameras, which have been used in interferometers made by 4D Technology since 2005, enable unprecedented temporal resolution in interferometer systems. The pixelated cameras have been used in many different types of interferometers including Twyman-Green, Fizeau, Self-Referencing, and Interference Microscopes. These systems have used multiple wavelengths as well as broadband sources. Data integration times as low as 10 nanoseconds have been achieved using a pulsed laser. The 4D Technology pixelated polarizer camera has been used primarily in commercial interferometers; however, the camera has excellent potential for polarimetry applications as shown in Figures 7 and 8. A sampling of phase data acquired with pixelated camera-based interferometers is shown in Figures 9, 10, 11, and 12.

Figure 7. Parsed pixelated camera polarization images shown on the left with two cars in the foreground and trees and shrubs in the background. On the right the corresponding DoLP image clearly discriminates the cars from the background scenery.

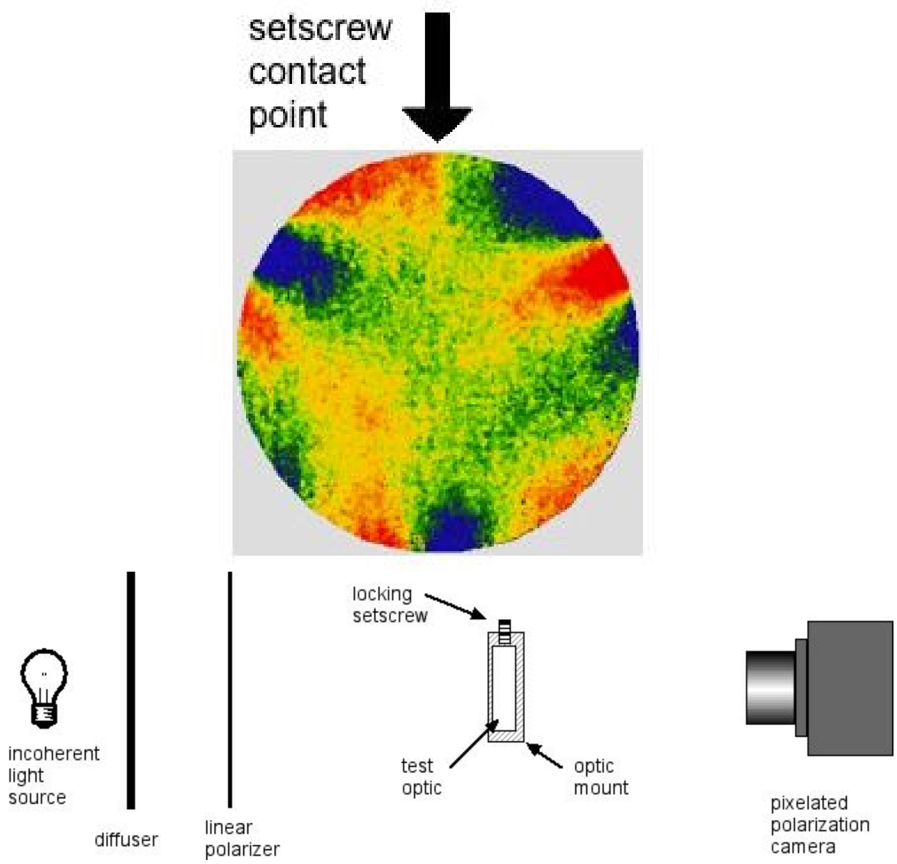

Figure 8. A one inch diameter substrate is stressed by its mounting set screw (represented by the arrow) in the phase image above which captures the resulting stress-induced birefringence. To capture the image, the simple setup diagramed above was used. Diffuse linearly polarized white light passes through the test optic and is captured by the pixelated camera. The peak-to-valley birefringence in the optic measured is 4nm/cm.

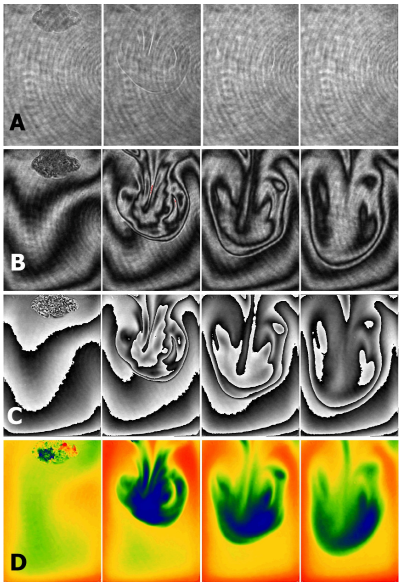

Figure 9. Phase-image frames of cold water drop dropped into cuvette of warm water. Object size is 20 x 35 mm taken at 0.1 sec intervals. (A) Bright field image. (B) Interference fringes. (C) Wrapped phase modulo 2π. (D) Phase images with a range (high-low) of 1.75 waves.

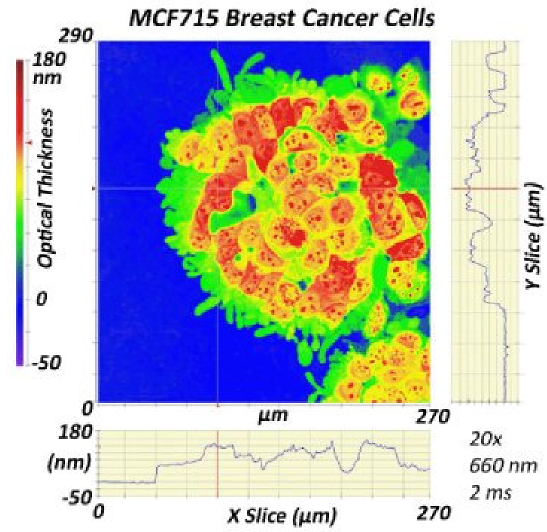

Figure 10. Phase image of breast cancer cell cluster captured with interference microscope using a 4D interference microscope.

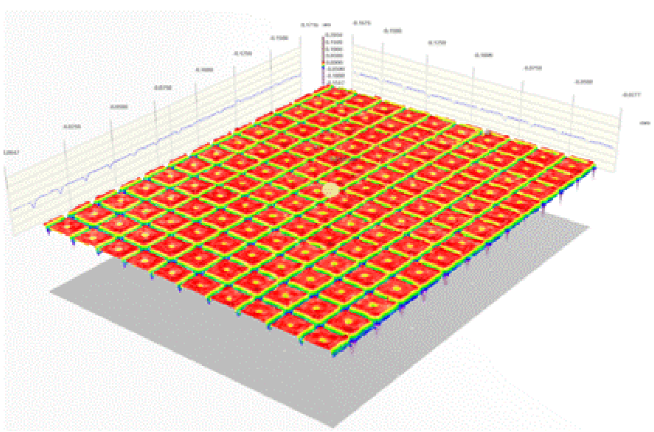

Figure 11. 3D image of MEMS micro-mirror device captured with multi-wavelength interferometer.

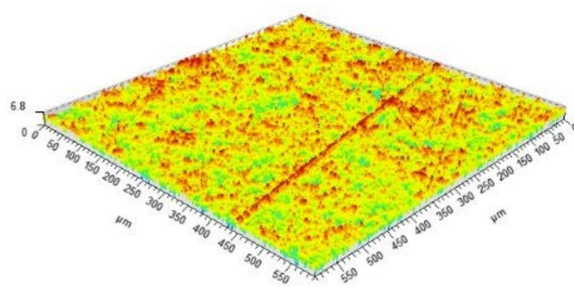

Figure 12. 3D mage of mirror surface captured with NanoCam surface roughness profiler.

6. CONCLUSIONS

High-resolution cameras employing micro-polarizer arrays were proposed over 16 years ago and are now in everyday use. The use of a solid state pixelated camera permits single shot acquisition of data that can freeze out motion and vibration, and enables high frame rate acquisition. Compared with multi-camera imaging systems, the pixelated camera approach is extremely compact and permits the use of high NA imaging systems with minimal requirements on clearance between the optics and the sensor. Novel processing algorithms can be used to achieve a spatial frequency response from the sensor that is nearly equal to the limit imposed by the finite pixel width. Wiregrid polarizer elements have desirable properties of high transmission, high extinction, and a broad spectral and angular bandwidth, making it possible to use them in applications spanning the visible and IR spectrum. The cameras can be configured to rapidly measure a wide variety of physical properties including, reflected, transmitted, and scattered polarization, birefringence, optical thickness, and surface shape. Given the commercial availability of these systems, it is anticipated that many other applications for the technology will be identified in years to come.

REFERENCES

[1] Chun, C. S. L., Fleming, D. L., Torok, E., J., "Polarization sensitive, thermal imaging," SPIE Vol. 2234, 275-286 (1994).

[2] Nordin, G. P., Meier, J. T., Deguzman, P. C., and Jones, M. W., "Micropolarizer array for infrared imaging polarimetry," J. Opt. Soc. Am A, 16(5), (1999).

[3] Millerd, J. E., Brock, N. J., Hayes, J. B., North-Morris, M., Novak, M., and, Wyant, J. C., "Pixelated phase-mask dynamic interferometer," Proc. SPIE Vol. 5531, 304-315 (2004).

[4] Tyo, J. S., Goldstein, D. L., Chenault, D. B., and Shaw, J. A., "Review of passive imaging polarimetry for remote sensing applications," Applied Optics, 45 (22), 5453-5469 (2006).

[5] Kimbrough, B.T., "Pixelated mask spatial carrier phase shifting interferometry algorithms and associated errors," Applied Optics 45(19), 4554–4562 (2006).

[6] Jones, M. W., Persons, C. M., "Performance predictions for micropolarizer array imaging polarimeters," Proc. SPIE Vol. 6682, 1-11 (2007).

[7] Moxtek Inc. Data Sheet: OPT-DATA-1005, Rev B.

[8] Kothiyal, P., and Delisle, R., "Shearing interferometer for phase shifting interferometry with polarization phase shifter," Applied Optics 24(24), 4439-4442 (1985).

[9] U. S. Patent No. US 7,230,717 B2

[10] Tyo, J. S., LaCasse, C. F., and Ratliff, B. M., "Total elimination of sampling errors in polarization imager obtained with integrated microgrid polarimeters," Optics Letters 34(20), 3187–3189 (2009).